International Journal of NanoScience and Nanotechnology.
ISSN 0974-3081 Volume 5, Number 2 (2014), pp. 133-150
© International Research Publication House
http://www.irphouse.com

A Review of Growth, Functionalization, and use of Graphene for Detection Applications

Ashok K. Sood, Isaac Lund and Yash R. Puri
Magnolia Optical Technologies, Inc. 52-B Cummings Park, Suite 314, Woburn, MA

Harry Efstathiadis and Pradeep Haldar
College of Nanoscale Science and Engineering (CNSE), Albany, NY 12222

Nibir K. Dhar
DARPA/MTO, 675 North Randolph Street, Arlington, VA 22203

Dennis L. Polla*
University of Minnesota, Minneapolis, MN 55455

Madan Dubey and Eugene Zakar
Army Research Laboratory, 2800 Powder Mill Road, Adelphi, MD 20783

Introduction

Graphene is a two dimensional analogue of graphite (carbon) material that has exceptional characteristics derived from the bonding characteristics of the C bonding sheets.

C has 4 valence electrons with 3 of these electrons participating in ů-bonding with its closest neighbors creating a honeycomb structure [1]. The 4th of these valence electrons occupy an orbital perpendicular to the one dimensional sheet creating delocalized ´-bonding as shown in Figure 1 that allows for the creation of a 2 dimensional electron gas (2DEG) creating high mobility within the sheets[1, 2].

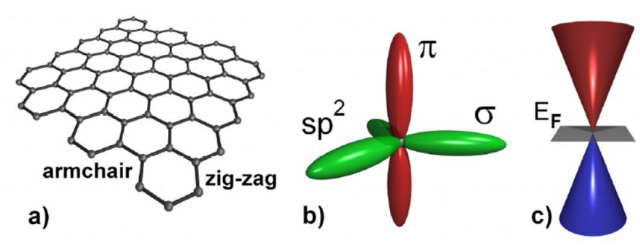

Figure 1: Graphene geometry as well and bonding and related band diagram [1]

The delocalization of the ´-bonding electrons allows for the graphene sheets to have high mobility up to 15000-200000 cm^2/Vs based upon the interference from the substrate, any contaminant particles, or from itself during bilayer growth [1, 3-7]. This makes cleanliness, grain size, and substrate interference a very important issue for the growing and use of graphene for high mobility and ultrafast applications.

The structure of graphene creates a semi-metal with a direct Fermi-Dirac band structure as shown in Figure 1 having charge carriers interact as direct Fermions (zero-effective mass) that allows for ballistic transport up to a micron at room temperature [8-10].This makes the replacement of Si by graphene for logic gates desirable due to the enabled switching speed that the high graphene mobility would enable, however the absence of a band gap means that one would have to be induced through a variety of doping mechanisms [11]. Several doping strategies as shown in Figure 2 have been proposed and tested including: electrostatic doping, chemical doping, and stress or geometry restricted doping by breaking the graphene periodicity (and band properties) [11].

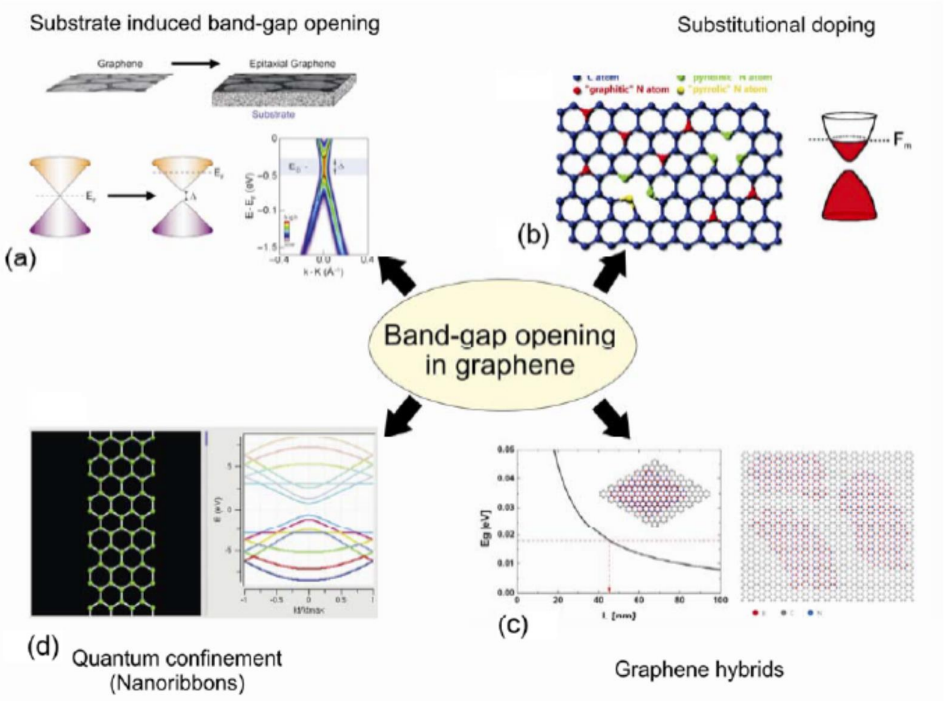

Figure 2: Diagram showing multiple mechanisms for inducing a band gap in graphene [25]

The induction of a band gap has been attempted by multiple groups creating transistors with low on/off ratio and high mobility with a tradeoff between on/off ratio and mobility possible through graphene functionalization techniques [1].This makes graphene more desirable for applications that require quick response but not

necessarily big on/off ratios such as radio-frequency (RF) electronics and infra-red (IR) detectors.

Graphene Fabrication:

Since grapheneôs performance is very susceptible to contamination and structural defects (such as folds, grain boundaries, and pin holes) from processing or transference a review of the graphene growth techniques should be attempted to determine the benefits and drawbacks of each [1]. Due to the sensitivity of graphene the growth must be chosen to be integrable with the required quality, processing, scale, and device architecture making exfoliation good for small test structure but inadequate for a repeatable semiconductor based process. As shown in Figure 3 there are three major pathways into creating graphene sheets either through exfoliation from bulk graphite, unzipping through etching a carbon nanotube, and the epitaxial growth from a gaseous or solid source.

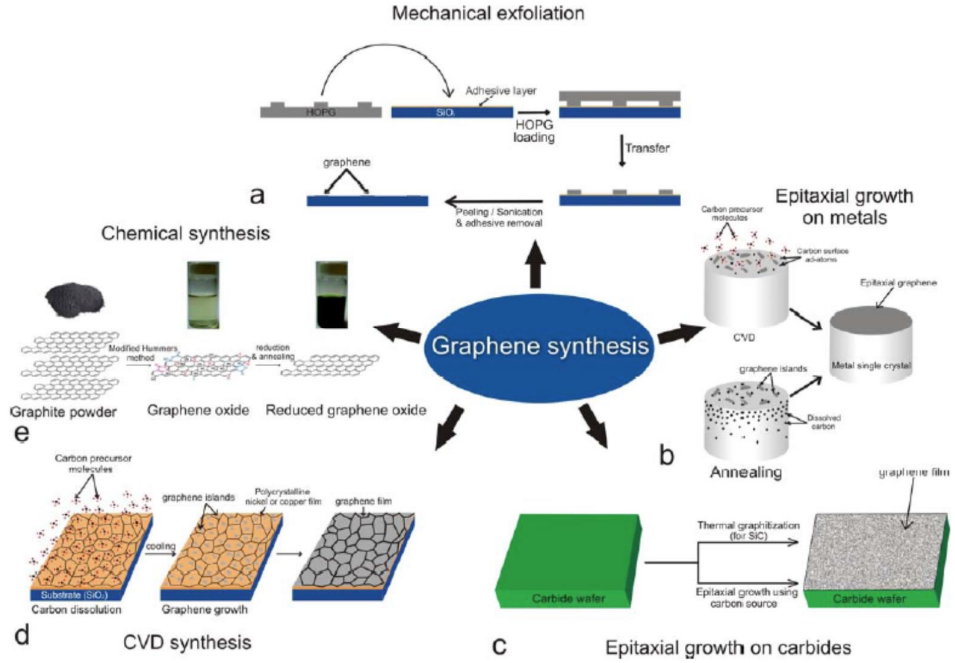

Figure 3: Fabrication schemes for the large scale synthesis of graphene sheets [25]

Exfoliation:

As of 2014 exfoliation produced graphene with the lowest number of defects and highest electron mobility with the founders of graphene Novoselov and Geim using the adhesive tape method to isolate graphene from graphite [1, 8, 12].The most common exfoliation method utilizes an adhesive tape to pull graphene films off a graphite crystal which are subsequently thinned down by further strips of tape and finally rubbed against the desired substrate.

This creates a random array of single, and double layer graphene flakes on the desired substrate that has been the driver for investigating the many properties of graphene, but since graphene is susceptible to creating folds during this process cannot be reproduced with high accuracy other mechanical and chemical exfoliation processes have been investigated. To address the difficulties of the scotch tape method one group tried to exfoliate graphene from highly ordered pyrolytic graphite (HOPG) utilizing a sharp single-crystal diamond wedge penetrates onto the graphite source to exfoliate layers [13]. This method has problems with defect initiation through shear stress and the reliable placement of the graphene flakes after exfoliation.

The other main exfoliation technique is to utilize liquid based techniques to create a dispersion of graphene or graphene oxide flakes that are drop casted or ink-jet printed and for the case with graphene oxide subsequently reduced. Liquid exfoliation can be accomplished through the use of solvents or ionic liquids with similar surface tension to graphene which when sonicated exfoliates the bulk graphite into graphene sheets which can be subsequently be centrifuged to create a supernatant and dispersed [14-17]. Probably the oldest known method for producing graphene is through the production of graphite oxide through the hummers method, sonicating to create a dispersion and then reduction of the graphene oxide either through the introduction of hydrazine at elevated temperature or through the introduction of a quick burst of energy introduced either through a light burst as shown in Figure 4 (flash or laser) or a temperature spike [13, 18, 19].

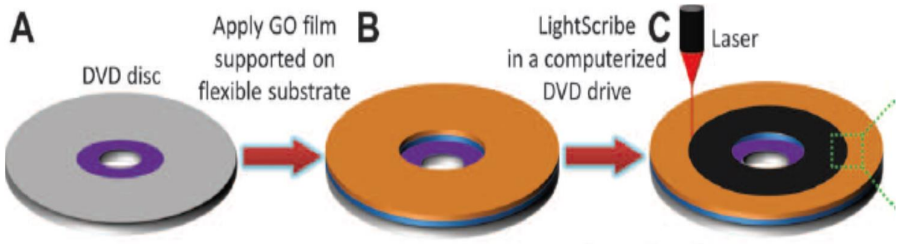

Figure 4: Reduction of graphene oxide using a LightScribe laser writing system ion a standard DVD writer [23]

One of the more interesting liquid exfoliation methods utilizes sonicating graphite at the interface of two immiscible liquids, most notably heptane and water, producing macro-scale graphene films [20]. The graphene sheets are adsorbed to the high energy interface between the heptane and the water, where they are kept from restacking [20]. The graphene remains at the interface and the solvents may then be evaporated isolating the graphene flakes [20].The utilization of mechanical exfoliation has produced very pristine flakes that have been beneficial in the investigation for the amazing characteristics of graphene, while the liquid exfoliation (and reduction) have been utilized for the production of transparent conducting oxides, conductive inks, and electrodes for Li-ion batteries and super capacitors. Mechanical exfoliation however has not been reliably scaled up to provide the reliable placement and large

graphene sheets desired for transistor and device applications.

Carbon nanotube unzipping:

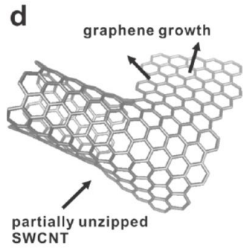

Figure 5: Image showing the unzipping of a carbon nanotube to produce graphene sheets [13]

As shown in Figure 5 graphene can be created by cutting open carbon nanotubes [7]. In one such method multi-walled carbon nanotubes are cut open in solution by action of potassium permanganate and sulfuric acid [21]. In another method graphene nanoribbons were produced by plasma etching of nanotubes partly embedded in a polymer film [21].This method is beneficial for the production of geometry restricted doping in graphene which will be addressed in the doping section of this paper. However the placement of the nanotubes on an integrable chip has been problematic and thus this method once again is only good for the production of test structures to probe graphene characteristics.

Epitaxy:

Epitaxy refers to the deposition of a crystalline overlayer on a crystalline substrate, where there is registry between the two. In some cases epitaxial graphene layers are coupled to surfaces weakly enough (by Van der Waals forces) to retain the two dimensional electronic band structure of isolated graphene [22, 23].There are three major ways of producing graphene epitaxially through the sublimation of Si from SiC, the precipitation of graphene from a carbide forming metal by controlling the cooling rate after deposition, and finally the production of graphene through the surface absorption of carbon on a non-carbide producing metal (such as Cu or Ir).

Heating silicon carbide (SiC), or other carbide materials (TaC, NbC, ZrC, HfC, TiC), to high temperatures (>1100 °C) under low pressures (~10^{-6} torr) boils off the Si (from either the Si face or underlying Si from the C face) and reconstitutes the C from the layer into a single layer graphene, although multi-layer graphene has been produced through this approach as well [25, 26]. This process produces epitaxial graphene with dimensions dependent upon the size of the wafer.

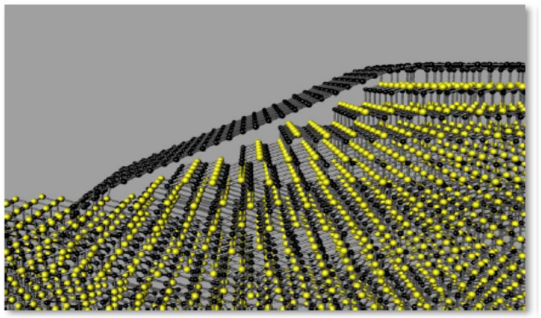

Figure 6: Bonding of graphene at a SiC step edge [27]

The face of the SiC used for graphene formation, silicon-or carbon-terminated, highly influences the thickness, mobility and carrier density of the resulting graphene, with the best results coming from a step edge in SiC that produces floating graphene that is attached to the SiC on the top and the bottom of the step edge as shown in Figure 6 [27].

There has also been some work utilizing Ni and Cu bilayer to catalyze the production of graphene from SiC achieving growth at higher pressures and lower temperature [28]. The benefit to using graphene produced from SiC is that SiC is easily integrable to a microelectronics technologies and processing, although it provides a higher band gap than is desired for most electronics applications providing a desire to transfer the graphene from its SiC substrate.

The precipitation of graphene from SiC also creates a Si_2O_3 insulating under layer which could assist with the transfer process and also that under high temperatures a large number of intercalant species can be placed between the graphene and SiC layer which can either help with the exfoliation or the electrical modification/isolation [25]. Under normal conditions the graphene SiC interface creates a Schottky contact, however it has been shown that the oxide can be transformed to a nitride under layer through a thermal annealing process in a nitride atmosphere modifying the electronic characteristics between the two [29].

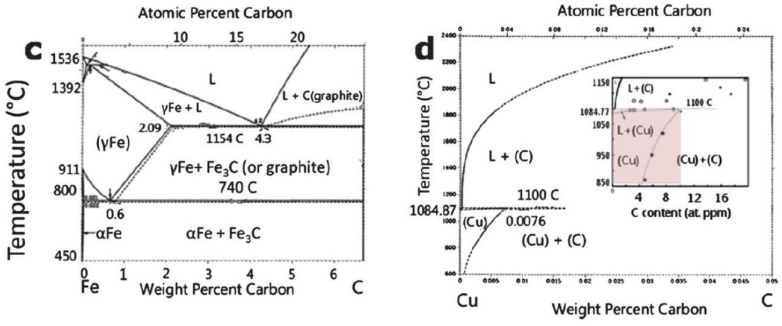

Figure 7: The phase diagram for carbide creating catalyst (Fe) and a non-carbide creating catalyst (Cu) [7]

Graphene growth utilizing a carbonaceous source material (such as methane introduced through a CVD process) differs from material to material with the carbon solubility in the metal and the growth conditions determining the deposition mechanism as shown by the phase diagrams in Figure 7 [7]. For carbide producing metallic substrates (such as Ni) graphene growth occurs through a precipitation process during cooling from the carbide [7]. The solubility of C in the metal (Ni for example) is higher at higher temperatures and thus during the furnace cooling phase carbon diffuses out of its Ni host [7]. The process of creating graphene from Ni creates a fundamental limitation of utilizing Ni as the catalyst is that single and few layered graphene is obtained over few to tens of microns regions and not homogeneously over the entire substrate [7]. The lack of control over the number of layers is attributed to the difference in out-diffusion of C from the grains and the grain boundaries of Ni creating non-homogeneous growth conditions.

In contrast to carbide producing metal catalysts, exceptional results in terms of uniform deposition of high quality single layered graphene over large areas have been recently achieved on polycrystalline copper foils [7]. The growth on Cu or Ir is simple and straightforward due to the metallic substrates not having a stable carbide material thus the decomposition of C is only reliant upon the grain orientation [30]. For example Cu is an FCC lattice with three dominant grain orientations Cu(100), Cu(110), and Cu(111) along with high index facets which are made up of combinations of low index facets [30]. Cu(100), Cu(110), and Cu(111) have cubic, rectangular, and hexagonal geometries making the Cu(111) grain orientation able to support epitaxial growth [30]. Thus grain growth on Cu(111) grains tend to be mono layered graphene sheets while Cu(100) and Cu(110) geometries prevent C diffusion causing compact multilayered C islands to form with higher index facets replicating the performance of the lower index grains [30].

Despite the ability for Cu and other metal substrates to grow good graphene flakes to make a usable device, graphene has to be transferred onto a semiconducting or insulating substrate [31]. The transference process usually involves spinning on a polymer, etching off the catalyst metal layer, then transferring the graphene onto the desired substrate by placing it on the substrate, and finally etching off the substrate [31]. Both of these processes can produce contaminants on the graphene layer reducing the mobility by adding scattering points in the sheet [1]. Groups have been working on ways to reliably reduce these contamination effects, one group has utilized Ti sputtering along with a Ti etch to remove any remaining Cu, while another group has shown that by first spinning on a lift off resist before a normal polymer backing layer produces a much cleaner graphene layer [32, 33]. High quality graphene has also been shown to be grown between a GaN and Ni interface where the Ni can be peeled off and the graphene layer is left on the GaN substrate [34].

Graphene doping:

Due to the chemical nature of the graphene with its zero band gap, mobility related to the delocalization of the ´-bonding orbitals, and lattice periodicity the doping of graphene can be achieved either through the breaking of lattice periodicity or the electrostatic confinement of the delocalized p_z orbitals [25]. There have been several

mechanisms proposed and tested that have been effective in shifting the Fermi energy either p or n type and the creation of p-n junction out of the interface [25]. It should be noted that by breaking the symmetry scattering is introduced into the graphene flake decreasing the mobility, which can also occur through electrostatic doping, so there is a general rule the higher the bandgap the lower the mobility.

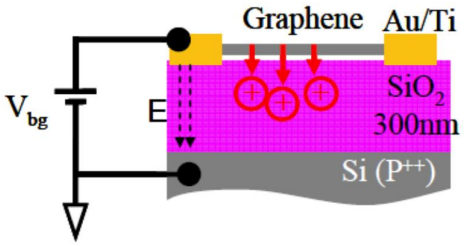

Figure 8: Image showing trapped charges at graphene oxide interfaces [35]

Also in terms of device integration since graphene is a self-contained sheet with no real interface layer it should be noted that process integration with oxide dielectrics as shown in Figure 8 can be difficult due to trapped impurities at the interface in terms of creating floating gates for voltage controlled variable gate transistors [35].

Electrostatic doping:

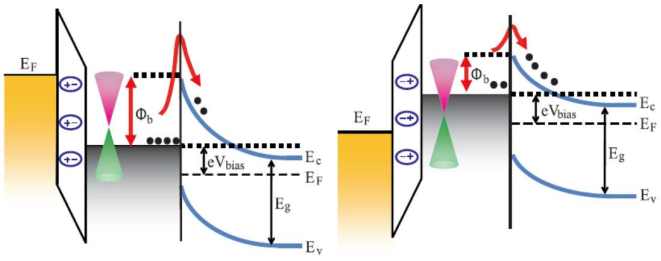

Figure 9: Diagram showing charge injection and Fermi modification of a graphene Schottky contact [36]

Electrostatic doping as shown in Figure 9 can be controlled through a variety of methods some with the use of floating gates with oxide buffer layers which allow for the voltage controlled operation of the graphene device creating a variable barrier and some with direct contact of the gating material [36]. Most electrostatic gating is accomplished through a horizontal device architecture to preserve the mobility of graphene making an ultrafast device. With both direct and indirect contact the electrostatic gating can be accomplished by utilizing metals with two different work functions, polymers with different end groups as shown in Figure 10, and finally layered materials with different opposing bandgaps with the higher bandgap being the acceptor and the lower being the donor as shown in Figure 11 [25]. Metals with

dissimilar work functions are normally integrated into a horizontal device with many different combinations to choose with the amount of gap opening being defined by the difference between the two metal work functions and the induced electric field weakening down the length of the sheet making the contact placement critical [37, 38].

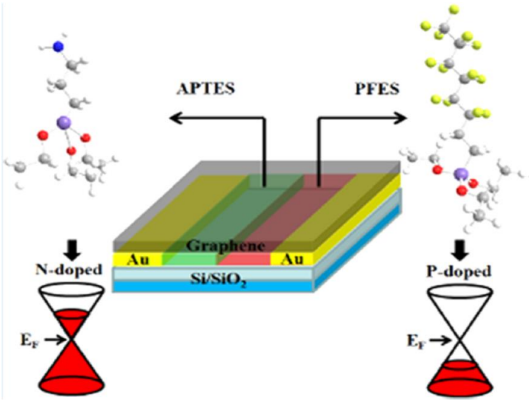

Figure 10: Diagram showing the doping of graphene utilizing different polymer end groups [11]

For polymers the use of different functional groups can electrostatically dope a horizontal graphene sheet with an isolated amine group (isolated nitrogen atom as in nitric acid) n-dopes the graphene sheet while fluorine is well known as a good electron acceptor so a polymer containing an isolated fluorine end group p-dopes the polymer as shown in Figure 10 [11]. For the polymer electrostatic doping technique similar atomic dopants are utilized for the chemical doping regime with atoms lower than group V providing n-type doping and elements higher then group V creating p-type dopants (this will create environmental sensitivity within an exposed graphene sheet due to the oxygen and hydroxide adatoms p-doping the graphene) [11, 39].

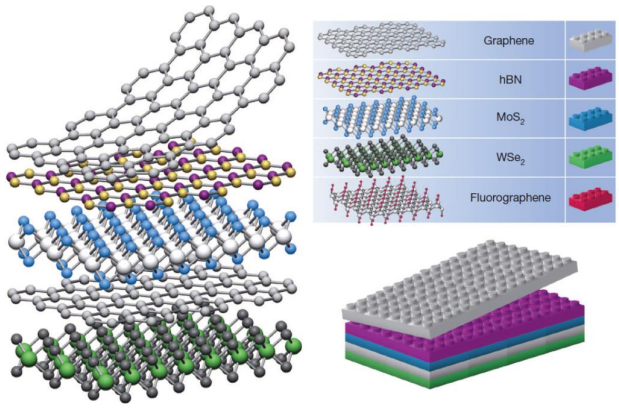

Figure 11: Diagram showing the stacking of multiple Van der Waals materials in order to create unique and tunable electrical properties [41]

Finally for electrostatic doping the utilization of other 2D materials as shown in Figure 11 can come into use with vertical device integration with either a homojunction based device or a heterojunction based device. For a homojunction based device graphene is utilized in a double layer with electrostatic doping coming from a layer above one graphene sheet with a lower band gap (such as tungsten diselenide WSe_2) and one below the other graphene sheet with a higher bandgap (such as molybdenum disulfide MoS_2) creating an electric field between the two 2D materials with different band gaps and electrostatically doping the graphene as shown in Figure 11 [40]. Since the electrostatic potential outside of a sheet with a bandgap will only induce a shift in the Fermi energy for graphene a heterojunction can be formed between the junction of the 2D materials with a tuning of the upper and lower contacts required [40]. The use of 2D stacked devices is interesting but it should be remembered that many of these layers have not been shown to be deposited one on top of the other requiring transfer techniques that can induce defects, transfer contaminants, and have arbitrary alignment between the lattices which can create different properties across the lattice due to misalignment as shown in Figure 12 [41, 42].

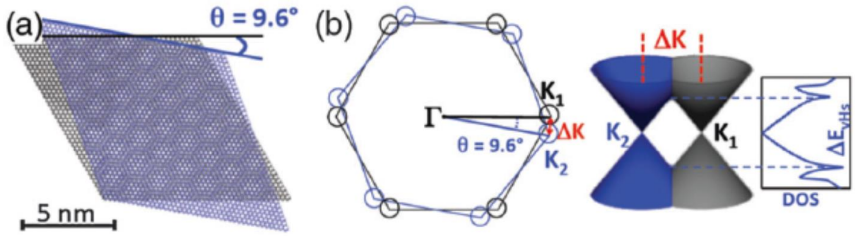

Figure 12: Image showing that the misalignment of 2D materials can electrically isolate the two sheets by separating the Dirac cones [52]

It has been shown that a twist angle of 2 graphene sheets above 2° electrically isolates the 2 graphene sheets from one another except at certain twist angles as shown in Figure 12 [42]. Most 2D materials have also been shown to have intrinsic doping due to vacancies and edge defects that create more problems for device integration [42].

Chemical doping:

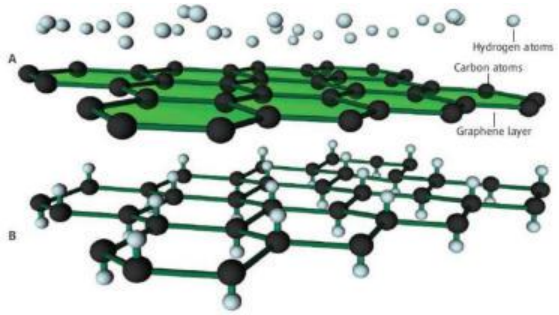

Figure 13: The functionalization scheme of graphene utilizing H_2 plasma [39]

As mentioned briefly in the electrostatic doping section chemical dopants can be utilized to modify the electrical characteristics of graphene and modify the Fermi energy to create p or n type doping as shown in Figure 13 [25, 39]. The mechanism is that the chemical dopant either bonds ionically or covalently to the delocalized p_z orbital [39]. This occurs either through the sharing of multiple delocalized electrons which weakly binds the adatoms onto the graphene sheet making them susceptible to segregating off with weaker bonding occurring according to the adatoms electronegativity [39].

The adatoms can also be ionically bonded to a single carbon atom breaking the symmetry creating a scattering defect and a bandgap opening [39, 43]. The amount of surface adatoms is reliant upon the dopant and the type of bonding with ionic bonding and larger electronegativity being able to obtain a stronger bond, higher dopant concentration, and higher band gap shifting [39]. However it should be noted that the higher the doping the more scattering and the lower the mobility, this leads chemical doping to be done on vertical devices with a small cross section and thus small diffusion length [25, 39].

Geometry restriction:

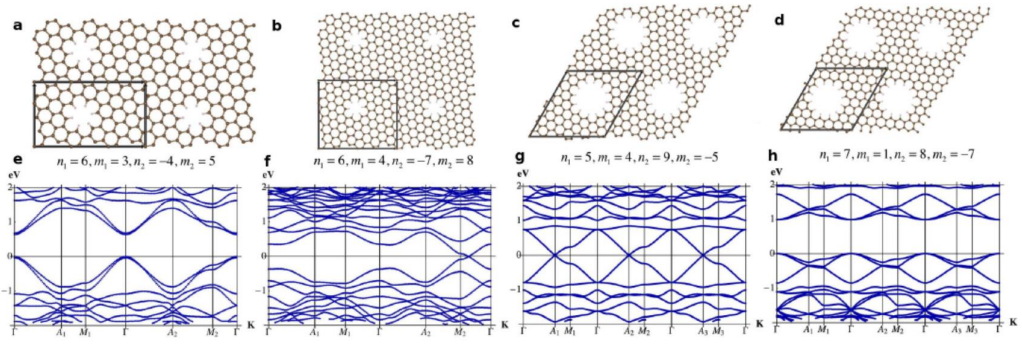

Figure 14: Different defined graphene sheet edge states and the associated band diagrams showing opening according to edge definitions [53]

The final way to dope graphene is by breaking the lattice periodicity of graphene as shown in Figure 14 [25, 44]. This can be done by reducing the size of a

graphene sheet in one direction so that the Fermi levels from the periodic boundary conditions are refined creating a quantum confinement effect [44]. Quantum confinement occurs when the materials dimensions are below the Bohr radius, which for graphene is at 10nm [25, 44]. This has been shown to be accomplished through the reduction of graphene into sheets with one dimension restricted under 10nm opening a gap of 2.5-3.0eV in theory and.5eV experimentally [25, 44].

Graphene with a size in either x or y under 10nm is known as a graphene nanoribbons and it suffers like many other graphene synthesis techniques from a lack of a reliable production technique [44]. Traditional semiconductor line definition techniques cannot reliably get a line definition below 20nm, with large problems creating lines with acceptable line edge roughness. For graphene the lack of line edge roughness is coupled with a lack of graphene conformality not knowing whether the line definition will create zig-zag or arm-chair end terminations which provide different conductivity values [25, 44]. The induced line edge roughness produces many scattering defect reducing the lattice periodicity and decreasing the mobility [25].

Utilizing graphene for IR detection:

Infrared (IR) detectors can be separated into two separate categories either thermal based IR detection or photon based detection as shown in Figure 15 [45].

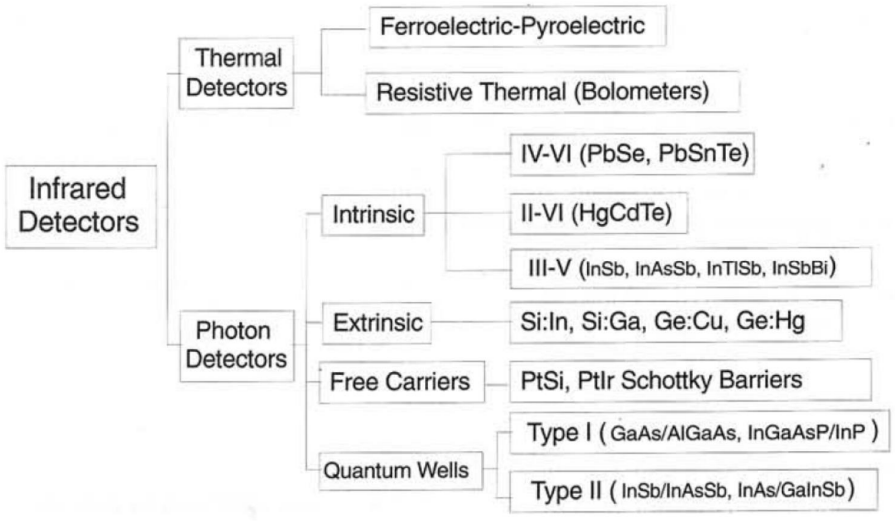

Figure 15: Categorization of IR detectors and currently utilized materials [45]

In thermal based detectors the incident IR radiation is absorbed raising the temperature of the material [45]. The raised temperature effects some temperature dependent property of the material for pyrometers this is a change in electrical polarization, while for bolometers this is a change in materials resistance [45]. Another more recent study utilized the photothermoelectric effect in graphene to create a net electric due to electron diffusion into dissimiliar metal contacts [38].

Photon based detectors utilize a band gap based detection with the arriving photon being absorbed and utilized to promote electron hole pairs to create a photocurrent [45].

The photon based detectors can be tuned to certain wavelengths by creating a quantum well structure [45]. Photon based IR absorbers are characterized by having quick absorption but usually require cooling due to thermal effects while thermal based IR detectors have high responsivity over a large wavelength and can be utilized at room temperature but are normally slow as shown in Figure 16 [45].

Detector type			Advantages	Disadvantages
Thermal			Light, rugged, reliable, & low cost Room temperature operation	Low detectivity at high frequency Slow response (ms order)
Photon	Intrinsic	IV-VI	Available low-gap materials Well studied	Poor mechanical property Large permittivity
		II-VI	Easy bandgap tailoring Well developed theory & exp.	Non-uniformity over large area High cost in growth and processing
		III-V	Good material & dopants Advanced technology Possible monolithic integration	Heteroepitaxy with large lattice mismatch
	Extrinsic		Very long wavelength operation Relatively simple technology	Extremely low temperature operation
	Free carriers		Low-cost, high yields Large & close packed 2-D arrays	Low quantum efficiency Low temperature operation
	Quantum wells	Type-I	Matured material growth Good uniformity over large area Possible 2-color detectors	Low quantum efficiency Complicated design and growth
		Type-II	Low Auger recombination rate Easy wavelength control	Complicated design and growth Sensitive to the interfaces

Figure 16: Advantage and disadvantages of currently utilized IR detectors [45]

This is where utilizing a graphene based sensing element is attractive due to the high mobility with little temperature sensitivity making it ideal for IR detectors [2].

Several groups have attempted to integrate graphene into IR detectors. The groups have tried both on the photon and the thermal based absorption methods [38, 46-51]. For photon based absorption methods the main focus has been the opening of a band gap through the geometric modification [38, 51]. One group utilized bilayer graphene to open a small band gap which is sensitive to thermalization requiring cooling to 5K for operation as shown in Figure 17 [51].

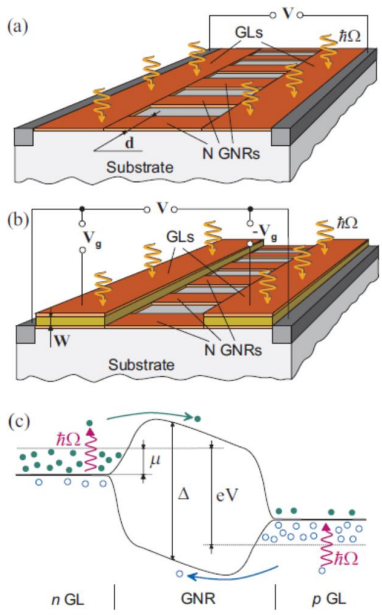

Figure 17: The utilization of graphene nanoribbons to open a small bandgap which is enhanced through the use of p and n type graphene contacts [38]

Another group utilized an array of aligned graphene nanoribbons to open up a small band gap which has significant difficulties in fabrication and noise properties from the nanoribbon edges [38].Groups that have tried thermal based IR detectors seem to have created more novelty, with one group multiple utilizing vertically aligned graphene flakes, while another group utilized a resonant structure of 2 graphene sheets separated by a dielectric to tune the photon wavelength of absorption as shown in Figure 18, and finally a group utilized the photothermoelectric effect as shown in Figure 19 to induce an electric current in graphene due to electric gating or dissimiliar metal contacts [38, 47, 50].

The bolometer utilizing vertically aligned graphene sheets utilized distance based tunneling between sheets for the bolometric effect, which is sensitive to contamination between sheets and alignment of the graphene flakes making reproduction difficult [50].

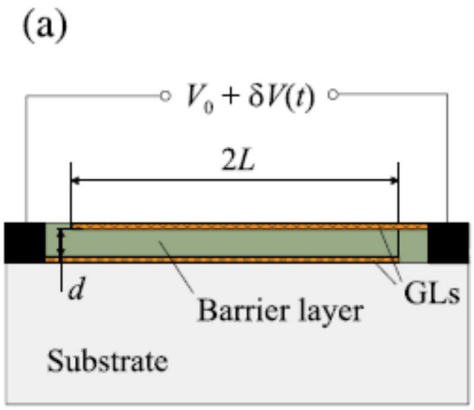

Figure 18: Phonon resonance based IR detector [47]

The resonance based IR detector as shown in Figure 18 utilizes the phonon resonance of two separate graphene sheets separated by a dielectric allowing for the tuning of wavelength detection based upon separation distance, but the production is difficult requiring pristine graphene and no trapped states in oxide which would both modify the resonant frequency and could possibly contaminate the detector out of detection range [47].

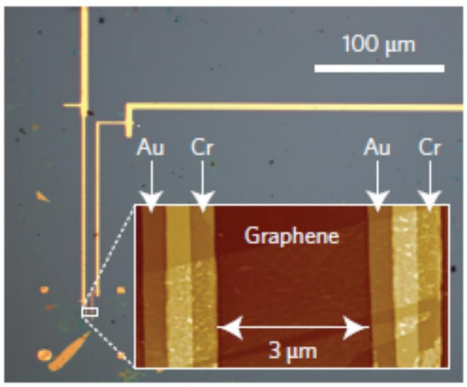

Figure 19: Image of a detector based upon the photothermoelectric effect [38]

The photo thermoelectric effect detector as shown in Figure 19 is relatively straight forward with contamination only affecting the speed of the detector and the noise only susceptible to trap states of the insulating oxide that the graphene is transferred onto [38].

In conclusion we have showed that the creation of graphene based IR detector is possible and can add many performance improvements to thermal IR based bolometric detectors. The growth and its consideration into the graphene quality as well as the device integration is discussed along with some of the state of the arts methods of directly integrating the grown graphene into devices is introduced. Finally

a brief discussion of graphene doping schemes is introduced for the creation of p-n junctions and electronic devices.

*Prof. Dennis L. Polla is currently with the Agency for Science, Technology and Research (A*STAR), 1 Fusionopolis Way, #18-01 Connexis North, Singapore 138632.

References:

[1] M. C. Lemme, Solid State Phenom. (2010) 156-158, 499
[2] H. Y. Hwang, Y. Iwasa, M. Kawasaki, B. Keimer, N. Nagaosa, and Y. Tokura, Nature Mater. (2012) 11, 103
[3] S.-Y. Kwon, C. V. Ciobanu, V. Petrova, V. B. Shenoy, J. Bare~no, V. Gambin, I. Petrov and S. Kodambaka, Nano Lett., 2009, 9, 3985.
[4] P. W. Sutter, J.-I.Flege and E. A. Sutter, Nat. Mater., 2008, 7, 406.
[5] J. Coraux, A. T. NôDiaye, C. Busse and T. Michely, Nano Lett., 2008, 8, 565.
[6] X. Li, W. Cai, J. An, S. Kim, J. Nah, D. Yang, R. Piner, A. Velamakanni, I. Jung, E. Tutuc, S. K. Banerjee, L. Colombo and R. S. Ruoff, Science, 2009, 324, 1312.
[7] C. Mattevi, H. Kim, and M. Chhowalla, J. Mater. Chem., 2011, 21, 3324
[8] A. H. C. Neto, F. Guinea, N. M. R. Peres, K. S. Novoselov and A. K. Geim, Rev. Mod. Phys., 2009, 81, 109.
[9] J.-H. Chen, C. Jang, S. Xiao, M. Ishigami and M. S. Fuhrer, Nat. Nanotechnol., 2008, 3, 206.
[10] X. Du, I. Skachko, A. Barker and E. Y. Andrei, Nat. Nanotechnol., 2008, 3, 491.
[11] H. Sojoudi, J. Baltazar, L. M. Tolbert, C. L. Henderson, and S. Graham, ACS Appl. Mater. Interfaces 2012, 4, 4781
[12] http://www.graphene.manchester.ac.uk/explore/the-story-of-graphene/a-discovery-at-manchester/
[13] Z. Yan, Z. Peng, G. Casillas, J. Lin, C. Xiang, H. Zhou, Y. Yang, G.Ruan, A. R. O. Raji, E. L. G. Samuel, R. H. Hauge, M. J. Yacaman, and J. M. Tour, J.ACS Nano, 2014, 140407122527007
[14] J. N. Coleman, M.Lotya, A. OôNeill, S. D. Bergin, P. J. King, U. Khan, K. Young, A.Gaucher, S. De, R. J. Smith, I. V. Shvets, S. K. Arora, G. Stanton, H.-Y. Kim, K. Lee, G. T. Kim, G. S. Duesberg, T. Hallam, J. J. Boland, J. J. Wang, J. F. Donegan, J. C. Grunlan, G. Moriarty, A.Shmeliov, R. J. Nicholls, J. M. Perkins, E. M. Grieveson, K.Theuwissen, D. W. McComb, P. D. Nellist, V.Nicolosi, Science, 2011, 331, 568
[15] P. Sutter, Nat. Mater. 2009, 8 (3), 171
[16] T. Ohta, A. Bostwick, J. McChesney, T. Seyller, K. Horn, and E. Rotenberg, Phys. Rev. Lett., 2007, 98 (20), 206802
[17] A. Bostwick, T. Ohta, J. L. McChesney, K. V. Emtsev, T. Seyller, K. Horn, and E. Rotenberg, New Jour. of Phys., 2007, 9 (10), 385.

[18] R. Mukherjee, A. V. Thomas, A. Krishnamurthy, and N.Koratkar, ACS Nano, 2012, 6 (9), 7867
[19] H. Feng, R. Cheng, X. Zhao, X. Duan and J. Li, Nature Commun. 2013, 4, 1539
[20] K. R. Paton, Nat. Mater. 2014, 13 (6), 624
[21] D. R. Lenski, and M.S. Fuhrer, Jour. of Appl. Phys., 2011, 110, 013720
[22] V. E. Calado, S.-E. Zhu, S. Goswami, Q. Xu, K. Watanabe, T. Taniguchi, G. C. A. M. Janssen, and L. M. K.Vandersypen, Appl. Phys. Lett., 2014, 104 (2), 023103
[23] M. F. El-Kady, V. Strong, S.Dubin, and R. B. Kaner, Science, 2012, 335 (6074), 1326
[24] Y. Hernandez, V. Nicolosi, M. Lotya, F. M. Blighe, Z. Sun, S. De, I. T. McGovern, B. Holland, M. Byrne, Y. K. Gun'Ko, J. J. Boland, P. Niraj, G.Duesberg, S. Krishnamurthy, R. Goodhue, J. Hutchison, V. Scardaci, A. C. Ferrari, and J. N. Coleman, J. N. Nat. Nanotech., 2008, 3 (9), 563
[25] D.Jariwala, A. Srivastava, and P.Ajayan, J.Nanosci.Nanotech.2011, 11 (8), 6621
[26] V. Alzari, D. Nuvoli, S. Scognamillo, M. Piccinini, E. Gioffredi, G. Malucelli, S. Marceddu, M. Sechi, V.Sanna, and A.Mariani, A. Jour. of Mater. Chem. 2011, 21 (24), 8727
[27] J.Baringhaus, M.Ruan, F.Edler, A. Tejeda, M.Sicot, A.Taleb-Ibrahimi, A.-P. Li, Z. Jiang, E. H. Conrad, C. Berger, C.Tegenkamp, and W. A. de Heer, Nature, 2014, 506, 349
[28] F.IacopiJour. of Mater. Research, Invited Feature Paper, in review (2014)
[29] J.Kunc, Y. Hu, J. Palmer, Z.Guo, J. Hankinson, S. H. Gamal, C. Berger, and W. A. de Heer, Nano Lett., 2014, 14 (9), 5170
[30] J. Lyding, J. Wood, and E. Pop, SPIE 2012 DOI: 10.1117/2.1201201.004110
[31] Y. Lee, S. Bae, H. Jang, S. Jang, S.-E. Zhu, S. H. Sim, Y. I. Song, B. H. Hong and J.-H.Ahn, Nano Lett., 2010, 10, 490.
[32] C. A. Joiner, T. Roy, Z. R. Hesabi, B. Chakrabarti, and E. M. Vogel, Appl. Phys. Lett., 2014, 104, 223109
[33] A. Nath, A. D. Koehler, G. G. Jernigan, V. D. Wheeler, J. K. Hite, S. C. Hernández, Z. R. Robinson, N. Y. Garces, R. L. Myers-Ward, C. R. Eddy Jr., D. K. Gaskill, and M. V. Rao, Appl. Phys. Lett., 2014, 104, 224102
[34] J. Kim, C.Bayram, H. Park, C.-W. Cheng, C.Dimitrakopoulos, J. A. Ott, K. B. Reuter, S. W. Bedell, and D. K. Sadana, Nat. Comm., 2014, 5, 4836
[35] H. Wang, Y. Wu, C. Cong, J. Shang, and T. Yu, ACS Nano, 2010, 4 (12), 7221
[36] H. Yang, J.Heo, S. Park, H. J. Song, D. H. Seo, K.-E.Byun, P. Kim, I. K.Yoo, H.-J. Chung, and K. Kim, Science, 2012, 336 (6085), 1140
[37] T. Mueller, F. Xia, andP.Avouris, Nat. Phot., 2010, 4, 297
[38] X.Cai, A. B. Sushkov, R. J. Suess, M. M. Jadidi, G. S. Jenkins, L. O. Nyakiti, R. L. Myers-Ward, S. Li, J. Yan, D. K.Gaskill, T. E. Murphy, H. D. Drew, and M. S. Fuhrer, Nat. Nanotech., 2014, 9, 814

[39] V.Georgakilas, M.Otyepka, A. B. Bourlinos, V. Chandra, N. Kim, K. C. Kemp, P. Hobza, R.Zboril, and K. S. Kim, Chem. Rev., 2012, 112 (11), 6156
[40] H. Tian, Z. Tan, C. Wu, X. Wang, M. A. Mohammad, D.Xie, Y. Yang, J. Wang, L.-J.Li, Jun Xu, and T.-L. Ren, Scien. Reports, 4, 5951
[41] A. K. Geim' and I. V. Grigorieva, Nature, (2013), 499, 419
[42] R.Bistritzer, and A. H. MacDonald, PNAS, 2011, 108 (30), 12233
[43] J.T. Robinson, J. S. Burgess, C. E. Junkermeier, S. C. Badescu, T. L. Reinecke, F. K. Perkins, M. K. Zalalutdniov, J. W. Baldwin, J. C. Culbertson, P. E. Sheehan, and E. S. Snow, Nano Lett. 2010, 10, 3001
[44] M. Y. Han, B.Özyilmaz, Y. Zhang, and P. Kim, Phys. Rev. Lett. 2007, 98, 206805
[45] M. Razeghi, Opto-Electron. Rev., 1998, 69(3), 155
[46] M.Freitag, T. Low, and P.Avouris, Nano Lett., 2013, 13 (4), 1644
[47] V.Ryzhii, T.Otsuji, M.Ryzhii, and M. S.Shur, J. Phys. D: Appl. Phys., 2012, 45, 302001
[48] X. Du, D. E. Prober, H. Vora, and C.Mckitterick, Graph.and 2D Mater., 2014, 1(1), 2299
[49] A. V. Klekachev, A.Nourbakhsh, I.Asselberghs, A. L. Stesmans, M. M. Heyns, and S. De Gendt, Electroch. Soc. Inter., Spring 2013, 63
[50] K. S.Hazra, N. Sion, A. Yadav, J.McLauhglin, and D. S.Misra, 2013, arXiv:1301.1302
[51] J. Yan, M-H. Kim, J. A. Elle, A. B. Sushkov, G. S. Jenkins, H. M. Milchberg, M. S. Fuhrer, and H. D. Drew, Nat. Nanotech., 2012, 7, 472
[52] W. Norimatsu, and M. Kusunoki, Phys. Chem. Chem. Phys., 2014, 16, 3501
[53] M. Dvorak, W. Oswald, and Z. Wu, Scien. Reports (2013), 3, 2289